6008 *Chem. Mater.* **2010,** *22,* 6008–6020
DOI:10.1021/cm1023025

CHEMISTRY OF MATERIALS
Article

Intralayer Cation Ordering in a Brownmillerite Superstructure: Synthesis, Crystal, and Magnetic Structures of Ca_2FeCoO_5

Farshid Ramezanipour,[†,‡] John E. Greedan,*[,†,‡] Andrew P. Grosvenor,[§] James F. Britten,[†,‡] Lachlan M. D. Cranswick,[∥] and V. Ovidiu Garlea[⊥]

[†]*Department of Chemistry, McMaster University, Hamilton, Ontario, Canada L8S 4M,* [‡]*Brockhouse Institute for Materials Research, McMaster University, Hamilton, Ontario, Canada L8S 4M,* [§]*Department of Chemistry, University of Saskatchewan, Saskatoon, Saskatchewan, Canada S7N 5C9,* [∥]*Canadian Neutron Beam Centre, National Research Council, Chalk River Laboratories, Chalk River, Ontario, Canada K0J 1J0, and* [⊥]*Neutron Scattering Sciences Division, Oak Ridge National Laboratory, Oak Ridge, Tennessee 37831, United States*

Received August 12, 2010. Revised Manuscript Received September 29, 2010

The synthesis, crystal, and magnetic structures and the bulk magnetic properties of Ca_2FeCoO_5, a brownmillerite type oxide, are presented. The crystal structure, solved and refined from single crystal X-ray and powder neutron diffraction data, is described in *Pbcm* with cell parameters, $a = 5.3652(3)$ Å, $b = 11.0995(5)$ Å, $c = 14.7982(7)$ Å. Thus, one axis, b in this setting, is doubled in comparison with the standard brownmillerite structure description giving rise to two sets of octahedral and tetrahedral sites. Aided by the strong scattering contrast between Fe and Co for neutrons, a nearly perfect intralayer cation site ordering, not observed for any brownmillerite before, is detected in the tetrahedral layers. There is a lesser degree of cation site ordering in the octahedral sites. Overall, the Fe/Co site ordering is of the NaCl type both within and between the tetrahedral and octahedral layers. There are also both intra- and interlayer ordering of tetrahedral chain orientations. The left- and right-handed orientations alternate within each tetrahedral layer as well as between the closest tetrahedral layers. The occurrence of the rare *Pbcm* space group in Ca_2FeCoO_5 is not consistent with a recently proposed structure-field map for brownmillerite oxides. The magnetic structure is G-type antiferromagnetic, with preferred orientation of magnetic moments parallel to the longest axis between 3.8 K to 100 K which switches to the shortest axis between 225 K and 550 K. The neutron diffraction data indicate different site specific ordering temperatures at about 450(5) K and 555(5) K. The refined ordered moments at 3.8 K are somewhat smaller than expected for Fe^{3+} and Co^{3+}(high spin) but are similar to those found in Sr_2FeCoO_5. There is evidence for spin canting from isothermal magnetization data that shows well pronounced hystereses and remnant magnetizations at 5 K and 200 K.

Introduction

Oxides with perovskite type structures exhibit a wide range of physical properties, making them strong candidates for both fundamental studies and technological applications. Colossal magnetoresistance, metal−insulator transitions, and superconductivity are just some of the interesting properties observed in these materials.[1−7] An understanding of the parameters that govern and control the structure and physical properties of these compounds can help to design materials with the properties desired for a particular application.

The formula of perovskite is ABO_3, where BO_6 octahedra condense to form a three-dimensional network of corner sharing octahedra with the A cations residing in the interstitial spaces. A number of perovskite based superstructures exist due to crystallographic ordering of for example cations on the A or B sites, $AA'B_2O_6$ or $A_2BB'O_6$, which have been studied extensively.[8−11] As well, superstructures exist in oxygen deficient perovskites with formula $A_2BB'O_5$, due to ordering of oxide vacancies. One of the most common superstructures of this type is that of brownmillerite, in which layers of corner sharing

*Corresponding author e-mail: greedan@mcmaster.ca. Corresponding author address: Department of Chemistry, McMaster University, Hamilton, Ontario, Canada L8S 4M1.

(1) Kobayashi, K.-I.; Kimura, T.; Sawada, H.; Terakura, K.; Tokura, Y. *Nature* **1998**, *395*, 677.
(2) Ramirez, A. P. *J. Phys.: Condens. Matter Phys.* **1997**, *9*, 8171.
(3) Kim, T. H.; Uehara, M.; Cheong, S. W.; Lee, S. *Appl. Phys. Lett.* **1999**, *74*, 1737.
(4) Tang, G. D.; Liu, X. M.; Li, Z. Z.; Hou, D. L.; Zhao, X.; Liu, L. H.; Qi, W. H.; Yu, Y.; Yu, R. C.; Jinphys, C. Q. *Stat. Sol.* (*a*) **2006**, *203*, 2522.
(5) Basith, M. A.; Manjura Hoque, Sk.; Shahparan, Md.; Hakim, M. A.; Huq, M. *Physica B* **2007**, *395*, 126.
(6) Imada, M.; Fujimori, A.; Tokura, Y. *Rev. Mod. Phys.* **1998**, *70*, 1039.
(7) Martin, L.O.-S.; Chapman, J. P.; Lezama, L.; Marcos, J. S.; Rodríguez-Fernández, J.; Arriortua, M. I.; Rojo, T. *Eur. J. Inorg. Chem.* **2006**, 1362.
(8) Anderson, M. T.; Greenwood, K. B.; Taylor, G. A.; Poeppelmeier, K. R. *Prog. Solid State Chem.* **1993**, *22*, 197.
(9) Howard, C. J.; Kennedy, B. J.; Woodward, P. M. *Acta Crystallogr.* **2003**, *B59*, 463.
(10) Karen, P.; Woodward, P. M. *J. Mater. Chem.* **1999**, *9*, 789.
(11) Chapman, J. P.; Attfield, J. P.; Molgg, M.; Friend, C. M.; Beales, T. P. *Angew. Chem., Int. Ed.* **1996**, *35*, 2482.

 Published on Web 10/14/2010

Table 1. Common Brownmillerite Space Groups and Their Different Settings

compound	$b > c > a$	$b > a > c$	$c > b > a$	$a > b > c$
$Ca_2Fe_2O_5$[16]	*Pnma*[a] [#62]	*Pcmn*		
Sr_2GaMnO_5[45]	*I2mb* [#46]	*Ibm2*		*Ima2*[a]
Sr_2FeCoO_5,[29] $Sr_2Fe_2O_5$[18]	*Imma*[a] [#74]	*Icmm*		
$La_{2-x}Sr(Ca)_xMn_2O_5$ (x = 0.7,0.8)[12]	*Pcmb* [#57]		*Pbcm*[a]	

[a] Denotes standard setting International Tables.

BO_6 octahedra are separated by chains of corner sharing $B'O_4$ tetrahedra.

The cell parameters of a brownmillerite are related to the perovskite structure in the following way: $a_b \approx \sqrt{2}a_p$, $b_b \approx 4a_p$, $c_b \approx \sqrt{2}a_p$. The most common space groups for typical brownmillerites are *Pnma*, *I2mb*, and *Imma*. These space groups refer to an unit cell setting where $b > c > a$. Various authors have chosen different settings of the unit cell leading to a variety of equivalent but somewhat confusing space group settings. Table 1 shows these common space groups and their different settings. The space groups of brownmillerite compounds are determined by the relative orientation of tetrahedral chains.[12−14] They can adopt two orientations that are mirror images of each other and are assigned arbitrary labels of left handed (L) and right handed (R). If all tetrahedral chains have the same orientation throughout the structure, the space group *I2mb* is obtained. If the long-range orientation is the same within a layer but opposite to the neighboring layer, *Pnma* results. There is also a much less common arrangement, previously observed only in $La_{1-x}A_xMnO_{2.5}$ (x = 0.2−0.4 for A = Sr, Ba and x = 0.2−0.3 for A = Ca)[12] consisting of both intra- and interlayer ordering of R and L chains which can result in the *C2/c* or *Pcmb* (*Pbcm*) space groups. Lastly, if chain orientations are long-range disordered, space group *Imma* occurs. In addition, a modulated distribution of tetrahedral chains has been suggested for $Ca_2Co_{2-x}Al_xO_5$, using the formalism of (3+1)-dimensional crystallography.[14] Also, local alternation of R and L chains within a layer has been studied for $Sr_2MnGaO_{4.97}$.[15] The intra- and interlayer chain configurations for *I2mb*, *Pnma*, and *Pcmb* are shown in Figure 1.

A number of oxygen deficient perovskites with Fe or Co on the B-site have been studied previously. $Ca_2Fe_2O_5$ is one of the well-known brownmillerite compounds which crystallizes in *Pnma*.[16] $Sr_2Fe_2O_5$ also has a brownmillerite structure, with two reported space groups *Ibm*2 (*I2mb*)[17] and *Imma* although it has been shown that the latter is correct.[13,18] Both Ca and Sr compounds can be synthesized using standard solid state methods. The long-range ordering of oxygen vacancies in both of these materials is accompanied by long-range antiferromagnetic ordering of spins.[17,18,19−21]

$Ca_2Co_2O_5$, with Co on the B-site, has been synthesized by different methods including thermal decomposition of solid-solution precursors, molten salt methods, and the citrate sol−gel process.[22−24] These methods were chosen to avoid problems associated with solid state synthesis of this compound, due to higher decarbonation temperature of the raw materials compared to the phase formation temperature.[23,24] The structure of this compound is not known in detail, but it is proposed to incorporate alternating square pyramidal and octahedral layers. Thermoelectric properties of this material have been of interest.[23−26] Recently, thin films of $Ca_2Co_2O_5$ deposited on a $NdGaO_3$ substrate by pulsed laser deposition were prepared.[27] Based on an electron microscopy study, the structure of the thin film was suggested to be brownmillerite type, with long-range ordering of O-vacancies and alternating octahedral and tetrahedral layers.[27] The Sr analogue, $Sr_2Co_2O_5$, has been studied as well. The crystal structure of this compound has been described as brownmillerite, *Ima*2 (*I2mb*), at room temperature.[28] However, it undergoes several structural phase transitions between room temperature and 1200 °C.[28]

It is also possible to mix both Fe and Co on the B/B′ sites. An *Icmm* brownmillerite structure has been assigned for Sr_2FeCoO_5 that was synthesized more than two decades ago.[29] Also, there have been reports of the formation of Ca_2FeCoO_5 as a result of thermal decomposition of carbonate or hydroxide precursors with unit cell dimensions a = 5.372 Å, b = 14.779 Å, and c = 11.123 Å and space group $P2_12_12_1$. Note the doubling of the c-axis.[22,30]

(12) Parsons, T. G.; D'Hondt, H.; Hadermann, J.; Hayward, M. A. *Chem. Mater.* **2009**, *21*, 5527.
(13) Greaves, C.; Jacobson, A. J.; Tofield, B. C.; Fender, B. E. F. *Acta Crystallogr., Sect. B: Struct. Crystallogr. Cryst. Chem.* **1975**, *31*, 641.
(14) Lambert, S.; Leligny, H.; Grebille, D.; Pelloquin, D.; Raveau, B. *Chem. Mater.* **2002**, *14*, 1818.
(15) Abakumov, A. M.; Rozova, M. G.; Pavlyuk, B. Ph.; Lobanov, M. V.; Antipov, E. V.; Lebedev, O. I.; Van Tendeloo, G.; Ignatchik, O. L.; Ovtchenkov, E. A.; Koksharov, Yu. A.; Vasil'ev, A. N. *J. Solid State Chem.* **2001**, *160*, 353.
(16) Berggren, J. *Acta Chem. Scand.* **1971**, *25*, 3616.
(17) Schmidt, M.; Campbell, S. J. *J. Solid State Chem.* **2001**, *156*, 292.
(18) D'Hondt, H.; Abakumov, A. M.; Hadermann, J.; Kalyuzhnaya, A. S.; Rozova, M. G.; Antipov, E. V.; Tendeloo, G. V. *Chem. Mater.* **2008**, *20*, 7188.
(19) Hirone, T. *J. Appl. Phys.* **1965**, *36*, 988.
(20) Takeda, T.; Yamaguchi, Y.; Tomiyoshi, S.; Fukase, M.; Sugimoto, M.; Watanabe, H. *J. Phys. Soc. Jpn.* **1968**, *24*, 446.
(21) Berasteguil, P.; Eriksson, S. G.; Hull, S. *Mater. Res. Bull.* **1999**, *34*, 303.
(22) Vidyasagar, K.; Gopalakrishnan, J.; Rao, C. N. R. *Inorg. Chem.* **1984**, *23*, 1206.
(23) Pei, J.; Chen, G.; Li, X.; Li, Y. X.; Zhou, N. *Mater. Lett.* **2009**, *63*, 1459.
(24) Liu, P. S.; Chen, G.; Pei, J.; Cui, Y.; Lu, D. Q.; Zhou, N.; Xian, H. Z. *Physica B* **2008**, *403*, 1808.
(25) Li, S.; Funahashi, R.; Matsubara, I.; Ueno, K.; Sodeoka, S.; Yamada, H. *J. Mater. Sci. Lett.* **2000**, *19*, 1339.
(26) Zhang, Y.; Zhang, J.; Lu, Q. *J. Alloys Compd.* **2005**, *399*, 64.
(27) Boullay, P.; Dorcet, V.; Pérez, O.; Grygiel, C.; Prellier, W.; Mercey, B.; Hervieu, M. *Phys. Rev. B.* **2009**, *79*, 184108.
(28) de la Calle, C.; Aguadero, A.; Alonso, J. A.; Fernández-Díaz, M. T. *Solid State Sci.* **2008**, *10*, 1924.
(29) Battle, P. D.; Gibb, T. C.; Lightfoot, P. *J. Solid. State Chem.* **1988**, *76*, 334.
(30) Gu, Z. J.; Xiang, X.; Li, F.; Liu, S. B.; Evans, D. G. *J. Phys. Chem. Solids* **2008**, *69*, 1056.

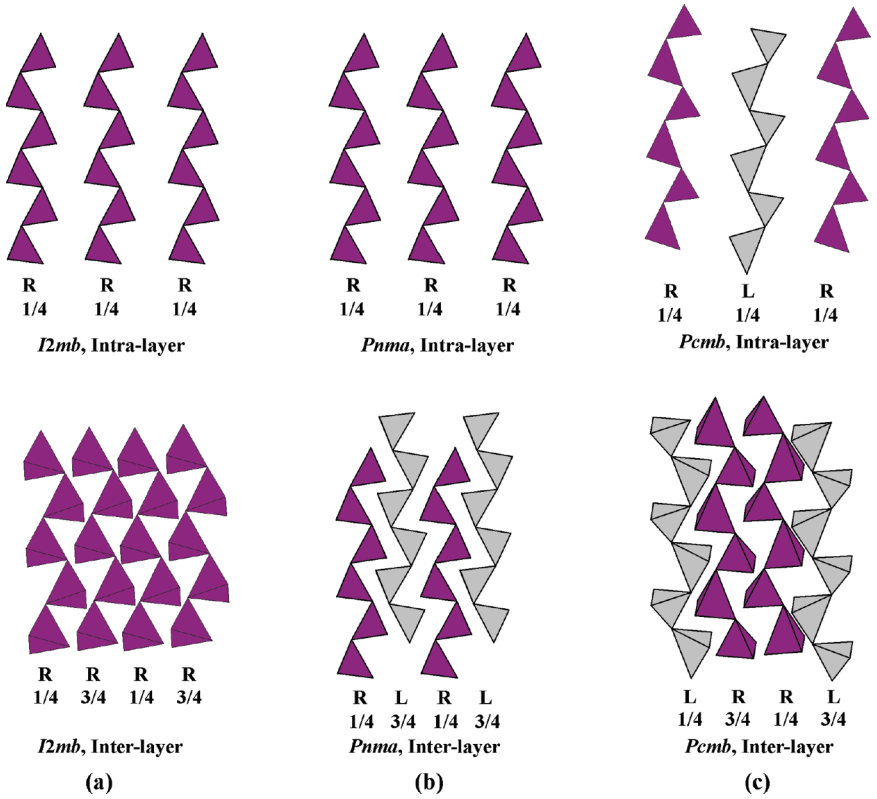

Figure 1. Schematic illustration of relative orientations of tetrahedral chains in brownmillerites. The common arrangements are shown in (a) and (b), while that for *Pcmb*, is shown in (c). The top figure in each shows the chain orientations in one tetrahedral layer, at $y = 1/4$, with the *a*-axis vertical and the *c*-axis horizontal. The bottom figure shows a view roughly along the *b*-axis for two layers at $y = 1/4$ and 3/4. In *I2mb*, (a), the chains have the same orientation within a layer and between the layers. In *Pnma*, (b), the chains have the same orientation within a layer but opposite orientation relative to the neighboring layer. In *Pcmb*, (c), the chains have opposite orientations relative to the neighboring chains within the same layer and in the adjacent layer.

In this paper, preparation of single crystals of Ca_2FeCoO_5 is reported. The availability of single crystals enabled solution of the structure by single crystal X-ray diffraction. Powder neutron diffraction data showed intralayer ordering of Fe and Co atoms between the tetrahedral sites which was not detected by X-rays. The bulk magnetic properties were studied from 5 K to 700 K. Neutron diffraction measurements were performed at several temperatures, from 3.8 K to 565 K, to determine the magnetic structure and show a temperature dependent spin reorientation.

Experimental Section

Synthesis. Accurately weighed $CaCO_3$ (99.99% Alfa Aesar), Fe_2O_3 (99.99% Alfa Aesar), and CoO (99.5% Cerac), with 4:1:2 molar ratio, were mixed and ground to fine powder. Pellets were made and sintered at 1100 °C in air for 24 h. The heating and cooling rates for this step and all subsequent refirings were 100 °C/hour. The sample (usually 1 to 2 g) was then reground and refired at 1200 °C in air for 48 h. After a final regrinding, the sample was sintered at 1250 °C in air for 48 h. Single crystals of Ca_2FeCoO_5 resulted from this procedure which proved to be suitable for single crystal X-ray diffraction studies. In all steps an alumina crucible covered by a platinum sheet was used as sample container.

X-ray and Neutron Diffraction. Single crystal X-ray diffraction data were obtained on a Bruker Mo Smart APEX2 diffractometer with a wavelength of 0.7107 Å and θ range of 2.76° to 45.34°. Limiting indices were $-10 < h < 10$, $-22 < k < 15$, and $-29 < l < 23$.

A PANalytical X'Pert Pro MPD diffractometer with a linear X'Celerator detector was used to obtain the powder X-ray diffraction data. The data were collected with a 2θ step interval of 0.0084° using CuKα_1 radiation ($\lambda = 1.54056$ Å).

Powder neutron diffraction measurements below 300 K were performed on the C2 diffractometer at the Canadian Neutron Beam Centre at Chalk River, Ontario. The data were collected at ten different temperatures from 3.8 K to 300 K. A wavelength of 2.373 Å with 2θ step size of 0.100° was used to collect data within the 2θ range of 4.4° to 83.6° and a wavelength of 1.331 Å with the same 2θ step size for the data from 34.9° to 114.6°. Neutron powder diffraction data above 300 K were collected using the HB2A diffractometer, at the High Flux Isotope Reactor at ORNL. Measurements were performed using an incident neutron wavelength of 2.41 Å, selected from the (113) plane of a vertically focusing Ge monochromator. A pyrolytic graphite (PG) filter was used to remove the higher order contamination of the beam. We used a 12′ Soller slit collimator in front of the monochromator and 21′ in front of the sample. The scattered neutrons were detected by an array of 44 equally spaced (~2.7°) ^{3}He detectors, each proceeded by a 6′ mylar foil collimator. For the data collection, the detector array was scanned to cover the total 2θ range of 8° to 130°, in steps of 0.05°. More details about the HB2A instrument and data collection strategies can be found in ref31. Powder samples weighing about 3 g were placed in vanadium cans (8 mm i.d. by 5 cm) and loaded in a Janis top-loading CCR capable of achieving temperatures up to 700 K.

(31) Garlea, V. O.; Chakoumakos, B. C.; Moore, S. A.; Taylor, G. B.; Chae, T.; Maples, R. G.; Riedel, R. A.; Lynn, G. W.; Selby, D. L. *Appl. Phys. A: Mater. Sci. Process.* **2010**, *99*, 531.

Magnetic Property Measurements. A Quantum Design MPMS SQUID Magnetometer was used to perform bulk magnetic measurements. The zero-field cooled and field cooled (ZFC/FC) magnetic susceptibility and isothermal magnetization data were obtained in the temperature range of 5 to 300 K on a powder sample in a gelatin capsule. The susceptibility data from 300 K to 700 K were obtained while heating the sample in a furnace using a quartz sample holder. Isothermal magnetization data from 0 to 5.5 T were also obtained at 5 K, 200 K, and 300 K.

Results and Discussion

Crystal Structure. Initially, a polycrystalline sample of Ca_2FeCoO_5 was studied using XRD data. The program GSAS[32] using EXPGUI interface[33] was used for refinement of the powder X-ray diffraction data. Refinements were attempted using the common space groups for brownmillerites, including *Pnma*, *Ibm*2, and *Imma* assuming the standard brownmillerite cell dimensions. However, in all cases there were extra peaks that could not be fitted to the models, indicating the possibility of a superlattice.

After synthesizing single crystals of Ca_2FeCoO_5, an X-ray single crystal study was performed. The X-ray reflections could be indexed on a cell, $a = 5.36750(10)$, $b = 11.1072(3)$, $c = 14.7787(3)$, that is, a supercell, two times the volume of that for a typical brownmillerite. Systematic absences were consistent with space group *Pbcm*. The program WinGX was used for solution and refinement of the single crystal structure.[34] The structure was initially solved in *P*1, and then symmetry was added so that all reflections could be explained using the highest symmetry. Table 2 shows the X-ray single crystal measurement results. These results confirm the larger cell reported in ref 26, but the correct space group, *Pbcm*, is now determined. Of course due to the very weak scattering contrast between Fe and Co using conventional X-rays, it was not possible to determine site preferences with confidence. It was found that a model with Fe on the tetrahedral sites and Co on the octahedral sites gave slightly smaller agreement indices and more satisfactory atomic displacement parameters as reported in Table 2. It should be noted that this space group, *Pbcm*, and unit cell, with one shorter axis doubled, is very rare among brownmillerite oxides, having been reported only quite recently for the materials $La_{2-x}Sr_xMn_2O_5$ and $La_{2-x}Ca_xMn_2O_5$ for $x = 0.70$ and 0.80.[12]

In a typical brownmillerite structure there are unique octahedral B and tetrahedral B′ sites arranged in layers parallel to the long axis. For cases with different B and B′ ions, interlayer site ordering is observed, for example Mn^{3+} and Cr^{3+} show a strong preference for the octahedral site in Ca_2FeMnO_5[35] and $Ca_2Fe_{1.5}Cr_{0.5}O_5$.[36] Ca_2FeCoO_5, however, has two inequivalent octahedral and tetrahedral sites (Figure 3). This structure type can thus accommodate both intra- and interlayer cation site ordering.

Table 2. X-ray Single Crystal Results for Ca_2FeCoO_5 at 293 K[a]

space group	*Pbcm*
lattice parameters	$a = 5.36750(10)$ Å
	$b = 11.1072(3)$ Å
	$c = 14.7787(3)$ Å
	$V = 881.08(3)$ Å^3
Z	8
agreement factors	$R(all\ data) = 0.0668$
	$wR = 0.0910$

atom	x	y	z	occupancy	U_{iso} (Å^2)
Ca1	−0.01196(7)	0.76115(6)	0.39239(4)	1	0.00978(10)
Ca2	−0.48847(7)	0.51099(6)	0.60752(4)	1	0.00967(10)
Fe1	0.44810(8)	0.71773(3)	0.2500	1	0.00661(7)
Fe2	−0.05003(8)	0.53219(3)	0.2500	1	0.00659(7)
Co1	−0.50320(5)	0.7500	0.5000	1	0.00754(11)
Co2	0.0000	1.000	0.5000	1	0.00657(11)
O1	0.0937(3)	0.68961(17)	0.2500	1	0.0088(3)
O2	0.5961(3)	0.56069(17)	0.2500	1	0.0090(3)
O3	−0.2538(3)	0.6240(2)	0.48463(9)	1	0.00883(18)
O4	−0.7545(3)	0.6260(2)	0.48888(9)	1	0.00978(19)
O5	0.0207(3)	0.4672(2)	0.36023(15)	1	0.0120(4)
O6	0.5125(3)	0.7823(3)	0.36033(17)	1	0.0135(4)

[a] Note that Fe and Co could not be distinguished by X-rays, but the following arrangement, with Fe on the tetrahedral sites and Co on the octahedral sites gave a slightly better agreement factor. For powder neutron diffraction results see Tables 3 and 4.

To answer questions concerning the details of the crystal structure, such as site preferences for Fe and Co, a powder neutron diffraction study was performed. There is good neutron scattering length contrast between Co ($b = 2.49$fm) and Fe ($b = 9.45$fm), while these two are virtually indistinguishable using conventional X-rays.

To determine the distribution of cations over tetrahedral and octahedral sites, different models were tested. The initial refinement was performed with Fe on both of the tetrahedral sites and Co on both octahedral sites which is the best result from the X-ray single crystal work, as mentioned. This resulted in very large agreement indices, with χ^2 values > 30 for the short wavelength data. The intensity of the (002) reflection was particularly underdetermined by this model. Detailed inspection of the refinement results showed very large thermal displacement factors, about 20 times larger than normal, for one of the tetrahedral sites, indicating that this site should be occupied fully or mostly by Co. There were also relatively large negative and positive displacement factors for the octahedral sites, indicating mixing of Fe and Co on these sites. Finally, a model with site ordering by Fe and Co over the two tetrahedral sites and mixing of Fe and Co on the octahedral sites was found to be the right model. The refinement profiles are shown in Figure 2b,c for the two wavelengths. For the $\lambda = 2.37150$ Å data set, the magnetic peaks, readily identified as those with a strong temperature dependence, were removed for structural refinement. The major magnetic peaks appeared at 31.0° and 31.7° with no structural overlap, along with smaller peaks at 60.6°, 60.9°, 62.2°, and 63.5°. The refinement results for Ca_2FeCoO_5 are given in Table 3. The unit cell parameters are compared to two typical brownmillerite

(32) Larson, A. C. ; Von Dreele, R. B. *General Structure Analysis System* (*GSAS*); Los Alamos National Laboratory Report LAUR; 1994, pp 86−748.
(33) Toby, B. H. *J. Appl. Crystallogr.* **2001**, *34*, 210.
(34) Farrugia, L. J. *J. Appl. Crystallogr.* **1999**, *32*, 837.
(35) Ramezanipour, F.; Cowie, B.; Derakhshan, S.; Greedan, J. E.; Cranswick, L. M. D. *J. Solid State Chem.* **2009**, *182*, 153.
(36) Battle, P. D.; Bollen, S. K.; Gibb, T. C.; Matsuo, M. *J. Solid State Chem.* **1991**, *90*, 42.

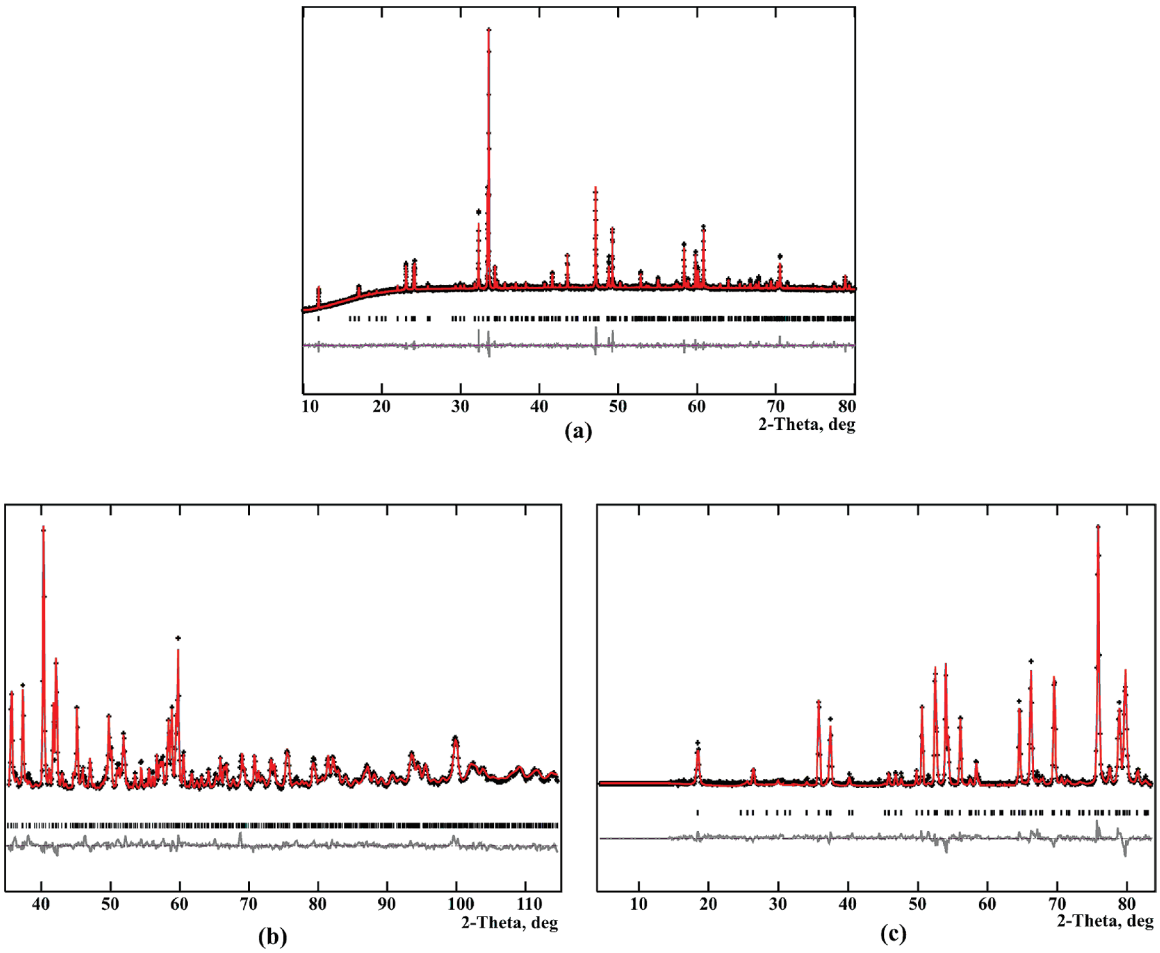

Figure 2. (a) X-ray powder diffraction refinement profile for Ca_2FeCoO_5, $\lambda = 1.54056$ Å, (b) neutron powder diffraction data $\lambda = 1.33037$ Å, and (c) neutron data $\lambda = 2.37150$ Å, at 300 K. The model is given in Table 4. For $\lambda = 2.37150$ Å data, the magnetic peaks were removed for structure refinement.

compounds, with similar compositions. Table 4 lists atomic coordinates and site occupancies for Ca_2FeCoO_5. Each atomic position for a typical brownmillerite splits into two sites due to the Ca_2FeCoO_5 super structure. The oxygen occupancies were refined, and no significant variation from full occupancy was observed. Therefore, it was decided to fix the oxygen occupancies at 1. Cation occupations at each site were constrained to 1 as well but not to the overall nominal bulk composition. We note a ~6.5% difference in overall cation composition between the Rietveld refinement results, $Ca_2Fe_{1.065}Co_{0.935}O_5$, and the nominal bulk sample composition, Ca_2FeCoO_5. It is not clear that this difference is significant given the limitations of Rietveld refinement of complex structures from powder data. What is clear is that the tetrahedral sites show nearly perfect Fe/Co site ordering, while the octahedral sites show lesser but still significant ordering levels.

Ca_2FeCoO_5 is the first example of a brownmillerite oxide showing intralayer ordering of cations. In addition, there is an interlayer ordering between octahedral and tetrahedral layers, so that an Fe-site in a tetrahedral layer is connected to Co-rich sites in the octahedral layers below and above. Similarly, a Co-site in a tetrahedral layer has Fe-rich sites as nearest neighbors in the adjacent octahedral layers. The overall pattern is that of NaCl (rock salt) ordering. This is illustrated in Figure 3c.

Tetrahedral site occupancies in Ca_2FeCoO_5 should be compared to those of Ca_2FeMnO_5 that has only one tetrahedral site, mostly occupied by Fe, with a 90%:10% ratio of Fe:Mn. This can be expected due to the difference between site preferences of Fe^{3+} and Mn^{3+}, with Mn^{3+} favoring the octahedral site. The two octahedral positions in Ca_2FeCoO_5 are jointly occupied by Fe and Co, with significantly more Fe content on one site and more Co content on the other, leading to a partial but substantial site ordering.

From previous K-edge XANES studies the cation oxidation states are Fe^{3+}/Co^{3+}.[37] Given the nearly even distribution of cations over the octahedral and tetrahedral layers, Co^{3+} must be high spin or at least intermediate spin as low spin Co^{3+} has a very strong octahedral site preference. The cation valences are also confirmed using bond valence sum (BVS) calculations.[38,39] For Fe1 and Co1 on the tetrahedral sites, the values are 2.88 and 2.846, respectively. For the octahedral sites, due to the mixed occupancies, an average value of BV parameters for Fe and Co was used, taking into account the percentages of each cation on each site. The BVS values obtained for the

(37) Grosvenor, A. P.; Greedan, J. E. *J. Phys. Chem. C* **2009**, *113*, 11366.
(38) Brown, I. D.; Altermatt, D. *Acta Crystallogr., Sect. B: Struct. Sci.* **1985**, *41*, 244.
(39) VALENCE program. /http://www.ccp14.ac.uk/ccp/web-mirrors/i_d_brown/S (accessed month day, year).

Table 3. Powder Refinement Results for Ca_2FeCoO_5 at 300 K[a]

	Ca_2FeCoO_5 (300 K)	Ca_2FeMnO_5 (550 K)	Sr_2FeCoO_5 (300 K)
space group	*Pbcm*	*Pnma*	*Icmm*
lattice parameters	a = 5.3652(3) Å b = 11.0995(5) Å c = 14.7982(7) Å V = 881.3(1) Å^3	a = 5.3251(1) Å b = 15.3865(3) Å c = 5.4787(1) Å V = 448.89(1) Å^3	a = 5.6243(2) Å b = 15.6515(5) Å c = 5.5017(2) Å V = 484.31 Å^3
Z	8	4	4
agreement factors	R_p (X-ray, λ = 1.54056 Å) = 0.0139 R_{wp} (X-ray, λ = 1.54056 Å) = 0.0262 R_p (neutron, λ = 1.33037 Å) = 0.0447 R_{wp} (neutron, λ = 1.33037 Å) = 0.0571 R_p (neutron, λ = 2.37150 Å) = 0.0441 R_{wp} (neutron, λ = 2.37150 Å) = 0.0573		

[a] The neutron refinements for the data with two wavelengths were done simultaneously. The X-ray refinement was done separately. The cell parameters for Ca_2FeMnO_5[35] and Sr_2FeCoO_5[29] are also shown for comparison.

Table 4. Atomic Coordinates, Site Occupancies, and Displacement Factors for Ca_2FeCoO_5 from Refinement of Neutron Diffraction Data at 300 K

atom	x	y	z	occupancy	U_{iso} (Å^2)
Ca1	−0.015(3)	0.759(1)	0.390(2)	1.0	0.018(7)
Ca2	−0.486(3)	0.512(1)	0.606(2)	1.0	0.013(5)
Fe1	−0.046(2)	0.533(1)	0.25	1.0	0.032(4)
Co1	0.426(7)	0.715(4)	0.25	1.0	0.002(8)
Co2	−0.496(3)	0.75	0.5	0.16(6)	0.027(7)
Fe2	−0.496(3)	0.75	0.5	0.84(6)	0.027(7)
Co3	0	0	0	0.71(5)	0.01(1)
Fe3	0	0	0	0.29(5)	0.01(1)
O1	0.099(4)	0.694(2)	0.25	1.0	0.031(6)
O2	0.591(4)	0.566(2)	0.25	1.0	0.021(5)
O3	−0.251(5)	0.622(2)	0.4830(6)	1.0	0.018(3)
O4	−0.755(4)	0.627(2)	0.4884(6)	1.0	0.016(3)
O5	0.020(2)	0.468(2)	0.362(1)	1.0	0.020(4)
O6	0.510(3)	0.782(2)	0.359(1)	1.0	0.018(4)

octahedral positions were 3.04 and 2.80 for Fe2(Co2) and Co3(Fe3) sites, respectively.

Table 5 shows selected bond distances and angles for Ca_2FeCoO_5. The two tetrahedral sites, Fe1 and Co1, have similar bond lengths and angles. Both FeO_4 and CoO_4 tetrahedra are highly distorted. In both cases the two bonds in the *a*-*b* plane are significantly longer than the bonds out of the plane. The extent of distortion of the tetrahedra is similar to that observed in the closely related compounds Ca_2FeMnO_5[35] and Sr_2FeCoO_5.[29] The tetrahedral bond angles in Ca_2FeCoO_5 show deviations from the ideal angle (109.5°). The largest deviations are observed for the angles that only involve O5 and O6 oxygen atoms. This is expected, as the bridging role of these oxygens between the tetrahedra and octahedra requires the occurrence of fairly irregular angles. Considering the similarity of bond distances and valences of Fe and Co in tetrahedral layer, their ordering is remarkable and puzzling.

The two octahedral sites in Ca_2FeCoO_5 show similar bond lengths, with elongation of the two out of plane bonds for both sites. For each octahedral site there are three pairs of equivalent bonds. For the Co3(Fe3) site, the octahedral site on the origin, all equivalent bonds are oriented opposite to each other, making 180° angles. This is due to the −1 point symmetry at the origin. However, for the other octahedral site, Fe2(Co2), where the point symmetry is only 2, the equivalent bonds within the *a*-*b* plane are oriented adjacent to each other, and the equivalent out of plane pair are opposite to each other with O−Fe−O angles deviating from linearity. The elongation of out-of-plane bonds for the octahedral sites occurs in regular brownmillerite compounds as well.[29,35] Such elongation seems to be required by this structure type in order to accommodate the linkage between octahedral and tetrahedral layers. Compression of tetrahedral out-of-plane bonds can accompany the elongation of octahedra. Also deviation from ideal angles for tetrahedral site bonds is much more pronounced compared to that of an octahedral site.

Schematic comparisons between the structure of a typical brownmillerite and the super structure of Ca_2FeCoO_5 are shown in Figures 3 and 4. The two distinct tetrahedral sites of Ca_2FeCoO_5 are particularly evident in Figure 3b. Viewed along the same direction, the tetrahedral site cations are completely eclipsed in a regular brownmillerite, while they have a significant shift relative to each other in Ca_2FeCoO_5. The shift of the octahedral cations is less pronounced. This is also evident from the atomic coordinates of octahedral and tetrahedral cations shown in Table 4.

The splitting of oxygens can also be seen in Figures 3 and 4. The oxygen atoms bridging the tetrahedral and octahedral layers are all of the same type and eclipse fully for a regular brownmillerite, while there are two different types of bridging oxygens, O5 and O6 for Ca_2FeCoO_5. However, the most pronounced case of two distinct oxygens that would be on the same site in a regular brownmillerite is seen for O1 and O2, as evident from Figure 4. This figure shows that the major difference between the Ca−O sublattices of a typical brownmillerite and Ca_2FeCoO_5 arises from the splitting of the O1 site, in a regular brownmillerite, into two sites labeled O1 and O2 in Ca_2FeCoO_5. Close inspection of the structure reveals that O1 and O2 are the oxygens bonded only to the tetrahedral cations with no connection to the octahedral ions. In fact, it appears that the symmetry of the octahedral layer does not deviate significantly from that of a regular brownmillerite, while the symmetry of the tetrahedral chains is the major factor that encourages formation of a super structure (Figure 3). As illustrated previously in Figure 1 the relative orientation of the

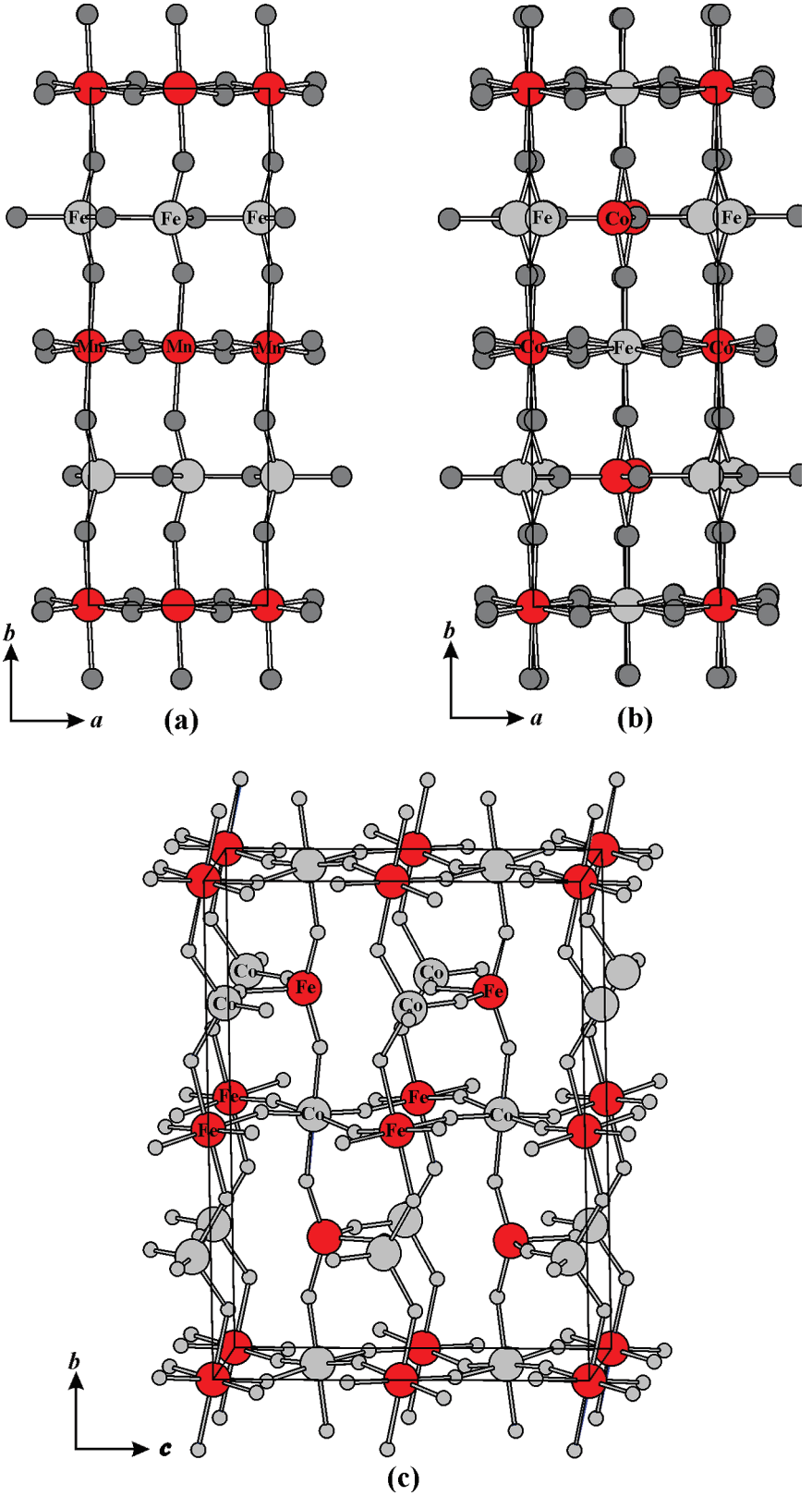

Figure 3. A comparison between (a) a regular brownmillerite structure Ca_2FeMnO_5 (*Pnma*)[35] and (b and c) the super structure of Ca_2FeCoO_5 (*Pcmb* setting is shown here, so that *a* and *b* are the shortest and longest axes in all three figures). In (a), there is only one octahedral B site, mostly occupied by Mn, and one tetrahedral B′ site, mostly occupied by Fe. Viewed along the *c* axis, all tetrahedral site cations are eclipsed. In (b), there are two octahedral sites, one occupied mostly by Fe and the other mostly by Co, and two tetrahedral sites, one fully occupied by Fe and the other by Co. The two distinct tetrahedral sites are especially evident in this figure. Also note that tetrahedral site cations are not eclipsed by the cations immediately behind them. In (c) the presence of both intra- and interlayer cation orderings, i.e., an overall NaCl type cation ordering is shown.

tetrahedral chains determines the space group symmetry of materials in brownmillerite family.

There have been a number of attempts to correlate brownmillerite space group symmetry to observable

Table 5. Selected Bond Lengths (Å) and Angles (°) for Ca_2FeCoO_5 at 293 K, Taken from Single Crystal X-ray Diffraction Data while the Site Occupations Are from the Neutron Data

tetrahedral sites	
Fe1−O1	1.9112(19)
Fe1−O2	1.9258(19)
Fe1−O5	1.822(2) × 2
Co1- O1	1.9276(18)
Co1−O2	1.9165(19)
Co1−O6	1.815(2) × 2
O1−Fe1−O2	104.34(9)
O1−Fe1−O5	106.18(8) × 2
O2−Fe1−O5	105.70(6) × 2
O5−Fe1−O5	126.80(15)
O1−Co1−O2	105.16(9)
O1−Co1−O6	104.60(6) × 2
O2−Co1−O6	106.30(8) × 2
O6−Co1−O6	127.96(17)
Fe1−O1−Co1	123.13(10)
Fe1−O2−Co1	123.95(10)
octahedral sites	
Fe2(Co2)−O3	1.950(2) × 2
Fe2(Co2)−O4	1.935(2) × 2
Fe2(Co2)−O6	2.097(2) × 2
Co3(Fe3)−O3	1.951(2) × 2
Co3(Fe3)−O4	1.929(2) × 2
Co3(Fe3)−O5	2.100(2) × 2
O3−Fe2(Co2)−O3	93.28(12)
O4−Fe2(Co2)−O4	91.60(12)
O3−Fe2(Co2)−O4	87.59(11) × 2
O3−Fe2(Co2)−O4	178.06(5) × 2
O3−Fe2(Co2)−O6	87.95(7) × 2
O3−Fe2(Co2)−O6	88.87(7) × 2
O4−Fe2(Co2)−O6	89.43(7) × 2
O4−Fe2(Co2)−O6	93.80(7) × 2
O6−Fe2(Co2)−O6	175.38(8)
O3−Co3(Fe3)−O3	180.000(1)
O4−Co3(Fe3)−O4	180.00(8)
O3−Co3(Fe3)−O4	87.41(11) × 2
O3−Co3(Fe3)−O4	92.59(12) × 2
O3−Co3(Fe3)−O5	92.58(7) × 2
O3−Co3(Fe3)−O5	87.42(7) × 2
O4−Co3(Fe3)−O5	90.35(7) × 2
O4−Co3(Fe3)−O5	89.65(7) × 2
O5−Co3(Fe3)−O5	180.000(1)
Fe2(Co2)−O3−Co3(Fe3)	166.59(7)
Fe2(Co2)−O4−Co3(Fe3)	170.18(8)

parameters, in particular the interlayer separation and degree of twisting of the tetrahedral chains.[12,40,41] The degree of chain twisting is a measure of the chain dipole moment, and the minimization of these moments is postulated to be responsible for the different chain configurations and thus the space groups. In ref 12, the most comprehensive and systematic study of brownmillerites to date, a structure field map was proposed based on these two parameters. The rare *Pcmb* (*Pbcm*) space group characterized by simultaneous intra- and interlayer ordering of chains is confined to the region where the tetrahedral layer separation exceeds ~8 Å, and the distortion of tetrahedral chains from linearity exceeds ~62°. However, for Ca_2FeCoO_5 the interchain separation is 7.41 Å and the average tetrahedral chain distortion angle is 56.5° which places this material within the *Pnma* region. The origin of this discrepancy is unclear at present but some observations may point the way to a resolution. Note that the *Pcmb* (*Pbcm*) region of the structure map relies on data from materials of composition $La_{1-x}A_xMnO_{2.5}$, containing the cations Mn^{3+} which is Jahn−Teller (JT) active and occupies the octahedral sites, and Mn^{2+} which resides on the tetrahedral sites. While all octahedral site cations in BM oxides exhibit a local tetragonal elongation along the *b* (longest axis), this effect is enhanced significantly for JT active ions as discussed for Ca_2FeMnO_5.[35] As well, Mn^{2+} (IV) has a very large effective radius, 0.66 Å compared to Fe^{3+}(IV) of 0.49 Å.[42] Both effects would act to enhance the *b*-axis length and, thus, the interchain separation. Indeed, the long axis dimensions reported for these materials lie in the range of 16−17 Å which is remarkable given the rather small radius of the A-site ions, ~1.2 Å for the combination $La_{0.6}Sr_{0.4}$ for CN = 8. In comparison the *b*-axis dimension for $Ba_2In_2O_5$ is 16.7 Å,[43] where both Ba^{2+}(CN = 8), 1.42 Å, and In^{3+}(CN = 6), 0.80 Å, (CN = 4), 0.62 Å have much larger radii than most of the ions involved here. Thus, the materials in which the rare *Pcmb* (*Pbcm*) space group and its unique chain configuration have been seen previously to this work may exhibit anomalously large *b*-axis lengths (and thus interchain separations) due to the presence of the strong JT ion Mn^{3+} and the large tetrahedral ion Mn^{2+}. Nonetheless, that Ca_2FeCoO_5 crystallizes in *Pcmb* (*Pbcm*) is still puzzling. It is not impossible that the Fe/Co tetrahedral site ordering plays a role. Note that tetrahedral Co^{3+} has the JT active configuration $e^3t_2^3$ which could drive a site preference. However, the bond distances for the two tetrahedral sites are similar, and also tetrahedral site ordering does not occur in Sr_2FeCoO_5,[29] which exhibits the random chain space group, *Imma*, suggesting that the A cation may play a subtle role.

Magnetic Structure. Neutron diffraction was used to determine the magnetic structure of this compound. The FullProf program,[44] employing WinPLOTR[45], was used to refine the neutron diffraction data. Figure 5 shows the refinement profile for crystal and magnetic structures of Ca_2FeCoO_5 at 3.8 K. The principal magnetic reflections, indexed as (022) and (102) on the chemical cell and marked with arrows, are diagnostic of the so-called G-type structure which is always found for brownmillerites with magnetic ions on both octahedral and tetrahedral sites. The G-type structure is shown in Figure 6 where the spins on each site are oriented antiparallel to those of all nearest neighbor sites within the same layer as well as in adjacent layers. The use of this nomenclature for brownmillerites, which was developed originally for

(40) Hadermann, J.; Abakumov, A. M.; D'Hondt, H.; Kalyuzhnaya, A. S.; Rozova, M. G.; Markina, M. M.; Mikheev, M. G.; Tristan, N.; Klingeler, R.; Büchnerd, B.; Antipov, E. V. *J. Mater. Chem.* **2007**, *17*, 692.
(41) Abakumov, A. M.; Kalyuzhnaya, A. S.; Rozova, M. G.; Antipov, E. V.; Hadermann, J.; Tendeloo, G. V. *Solid State Sci.* **2005**, *7*, 801.
(42) Shannon, R. D. *Acta. Crystallogr., Sect. A: Cryst. Phys., Diffr., Theor. Gen. Crystallogr.* **1976**, *32*, 751.
(43) Gregory, D. H.; Weller, M. T. *J. Solid State Chem.* **1993**, *107*, 134.
(44) Roisnel, T.; Rodriguez-Carvajal, J. *FULLPROF ver 1.9c: Rietveld, Profile Matching & Integrated Intensity Refinement of X-ray and/or Neutron Data*; Laboratoire Léon Brillouin: Saclay, France, 2001.
(45) Roisnel, T.; Rodríguez-Carvajal, J. WinPLOTR: a Windows tool for powder diffraction patterns analysis. In *Proceedings of the Seventh European Powder Diffraction Conference* (*EPDIC 7*); Delhez, R., Mittenmeijer, E. J., Eds.; Materials Science Forum, 2000; pp 118−123.

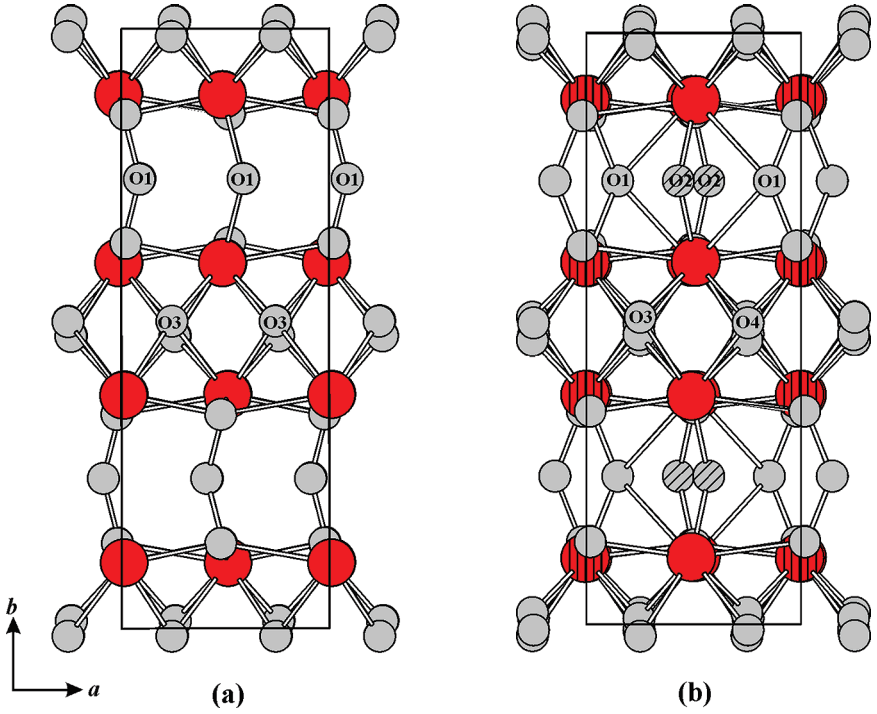

Figure 4. The Ca−O sublattices of (a) a regular brown millerite structure Ca_2FeMnO_5 (*Pnma*)[35] and (b) the super structure of Ca_2FeCoO_5 (*Pcmb* setting is shown here, so that *a* and *b* are the shortest and longest axes in both parts (a) and (b) of the figure). In (a) Ca cations (large red circles) are arranged in layers that have only one type of oxygen on each side (O1 on one side and O3 on the other side). In (b) two oxygen positions are present on each side of a Ca-layer. The pronounced distinction between O1 and O2 is especially evident in this figure. There are two types of Ca positions. Ca1 is vertically hatched to be distinguished from Ca2.

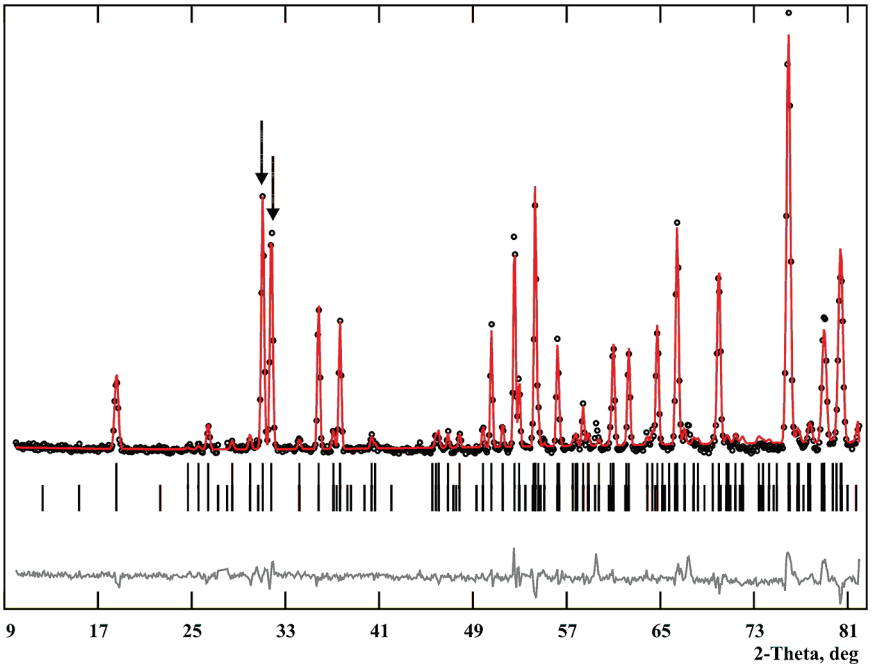

Figure 5. Crystal and magnetic structure refinement profile of neutron powder diffraction data for Ca_2FeCoO_5, $\lambda = 2.37150$ Å, at 3.8 K. The black circles are the experimental data; the solid line is the model; two rows of the vertical bars show Bragg peak positions for the crystal (top) and magnetic (bottom) structures, and the lower line is the difference plot. The two major magnetic peaks are shown by arrows. The magnetic structure was found to be G-type with the preferred moment orientation along the longest axis (*b* in *Pcmb* setting) at 3.8 K.

perovskites - which have only octahedral sites - can lead to ambiguities, so some brief remarks are in order. Note from Figure 6 that the spin configuration for the octahedral sites (or the tetrahedral sites) taken alone is actually what is called C-type in perovskites. This is why the indices of the strongest magnetic reflections are (022) and (102) which are those expected for a perovskite C-type.[46] Nonetheless, when the two sites are taken

(46) Pomjakushin, V. Yu.; Balagurov, A. M.; Elzhov, T. V.; Sheptyakov, D. V.; Fischer, P.; Khomskii, D. I.; Yushankhai, V. Yu.; Abakumov, A. M.; Rozova, M. G.; Antipov, E. V.; Lobanov, M. V.; Billinge, S. J. L. *Phys. Rev. B* **2002**, *66*, 184412.

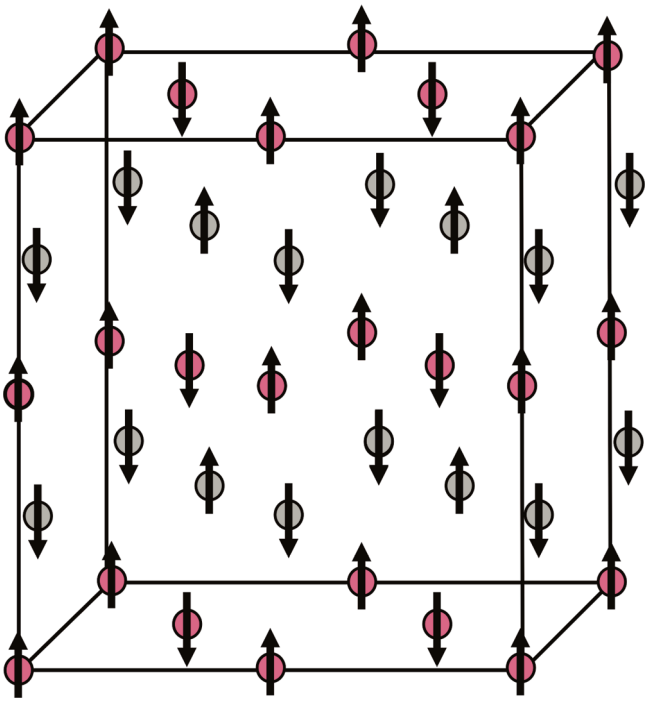

Figure 6. The G-type magnetic structure of Ca_2FeCoO_5 at 3.8 K (cell setting $b > c > a$, chemical space group *Pcmb*). The octahedral and tetrahedral cations are shown in red and grey, respectively. The magnetic moment on each site is aligned antiferromagnetically relative to all nearest neighbors within the same layer and in the adjacent layers. Note that the octahedral and tetrahedral site components, taken separately, are actually C-type. Thus, an alternative description would be as two interpenetrating C-type magnetic structures.

together, all nearest neighbor moments are indeed antiparallel which is the situation for a G-type magnetic structure and such nomenclature has been adopted for brownmillerites. Regarding the orientation of magnetic moments, the intensity ratio of the (022)/(102) doublet is also diagnostic. Simulations show that for moment orientation along the longest axis (*b* in this case) the (022)/(102) intensity ratio is 1.2. For orientation along the shortest axis (*a*-axis in this case and in most settings for the brownmillerite cell) the ratio is 2.9. For orientation along the third axis the intensity ratio is 0.4. In Figure 7a,b are plotted the temperature dependences of the individual intensities and the ratio. Note the highly unusual behavior with temperature of the individual reflection intensities (7a) and the results of 7b which indicate clearly a spin reorientation from along the *b*-axis between 3.8 K and 100 K to along the *a*-axis by about 200 K which remains unchanged to 502 K, although the errors are larger in the data for $T > 300$ K. Most Fe-based brownmillerites show a preferred moment direction along the shortest (a) axis such as $Ca_2Fe_2O_5$,[47] $Sr_2Fe_2O_5$,[48] $Ca_2Fe_{1.5}Cr_{0.5}O_5$[36], and Sr_2FeCoO_5,[29] although for the latter the magnetic structure is known only at room temperature. Only Ca_2FeMnO_5 shows a preferred moment direction along the longest axis (*b*) at all temperatures. It is worth noting that the Mn^{3+}-based brownmillerites Ca_2GaMnO_5 and Sr_2GaMnO_5[46] also have a preferred *b*-axis at all temperatures, indicating a strong anisotropy associated with the Mn^{3+} ion. $Ca_2Co_{1.6}Ga_{0.4}O_5$ with Co^{3+} on both octahedral and tetrahedral sites takes the *a*-axis at 298 K. [49] Clearly, more work is needed to understand the systematics of magnetic anisotropy in brownmillerites.

The preferred directions deduced from Figure 7b were confirmed by magnetic structure refinements which converged only when the moment directions for all four sites were taken as indicated. The refined magnetic moments for all four crystallographic sites for the two regions up to 300 K are listed in Table 6. Note that the uncertainties of the moments are rather large. In fact comparing these values to those obtained for the simpler Ca_2FeMnO_5 material from the same diffractometer over the same Q-range, the uncertainties range from twice (at low temperature) to three or four times (at high temperature).[35] This is likely due to the fact that the number of magnetic reflections is actually the same for both materials, while the number of magnetic sites has doubled.

The same effect appears for the chemical structure refinement where the uncertainties in atomic positions for Ca_2FeCoO_5 are significantly larger than those for $CaFeMnO_5$. Again, the data span the same Q-range, but the model contains twice as many atoms for the doubled cell material. Thus, the least-squares landscape for Ca_2FeCoO_5 appears to consist of many shallow minima.

Given this problem it is not surprising that the refined moment magnitudes were found to be remarkably sensitive to the refinement strategy. For the data taken at the C2 diffractometer encompassing the temperature range 3.8 K to 300 K, full data sets (both wavelengths) were available only for the two terminal temperatures while for all others only the long wavelength data exist. It was, thus, not possible to refine atomic positions and moments simultaneously at all temperatures. The best results (in terms of R_{mag}) were obtained when the atomic positions found at 3.8 K from the neutron data were used to refine the magnetic moments at 3.8 K, 50 K, and 100 K, and those found from the 300 K refinement were used for the 225 K, 250 K, 275 K, and 300 K, and these are the values listed in Table 6. In all cases an overall displacement parameter, B_{ov}, was refined. The obtained magnetic moments are generally smaller than what is expected for Fe^{3+} (d^5, $S = 5/2$) and high spin Co^{3+} (d^4, $S = 2$). Low magnetic moments comparable to those reported here have been observed previously for Sr_2FeCoO_5.[29] Further speculation regarding the origin of these apparent discrepancies is unwarranted at this time. The use of core level spectroscopies to determine the spin state of the Co ions for example may prove helpful.

(47) Takeda, T.; Yamaguchi, Y.; Tomiyoshi, S.; Fukase, M.; Sugimoto, M.; Watanabe, H. *J. Phys. Soc. Jpn.* **1968**, *24*, 446.
(48) Takeda, T.; Yamaguchi, Y.; Watanabe, H.; Tomiyoshi, S.; Yamamoto, H. *J. Phys. Soc. Jpn.* **1969**, *26*, 1320.
(49) Istomin, S. Ya.; Abdyusheva, S. V.; Svensson, G.; Antipov, E. V. *J. Solid State Chem.* **2004**, *177*, 4251.

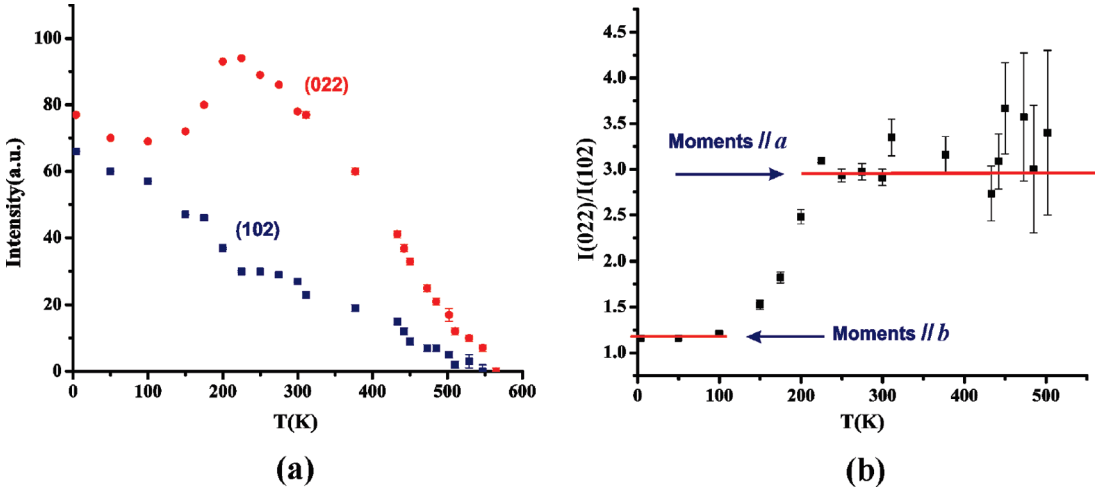

Figure 7. (a) Temperature dependence of two major magnetic reflections for Ca_2FeCoO_5 (*Pcmb*) at 31.06° indexed as (0 2 2) and 31.80° indexed as (1 0 2). The unusual changes in relative intensities below 300 K are due to spin reorientation as a function of temperature. Note the presence of plateau near 450 K and 500 K. (b) The ratio of (0 2 2)/(1 0 2) peak intensities as function of temperature. For ratios close to 1, below 100 K, the moments are parallel the longest axis, *b*-axis, and for ratios close to 3, above 225 K, the moments point along the shortest axis, *a*-axis in *Pcmb* setting.

Table 6. Refined Magnetic Moments for Ca_2FeCoO_5[a]

temperature moments' orientation	3.8 K *b*-axis	50 K *b*-axis	100 K *b*-axis	225 K *a*-axis	250 K *a*-axis	275 K *a*-axis	300 K *a*-axis
Fe1(Td)	3.1(2)	3.2(3)	3.1(2)	2.7(5)	2.4(6)	2.0(4)	2.4(4)
Co1(Td)	2.8(2)	2.7(2)	2.7(2)	2.9(5)	2.8(6)	2.9(4)	2.4(3)
Fe2(Co2)(Oct)	3.6(3)	3.5(3)	3.7(2)	3.1(5)	2.7(6)	2.1(4)	2.8(4)
Co3(Fe3)(Oct)	2.3(2)	2.3(3)	2.1(2)	2.2(5)	2.2(7)	2.6(4)	1.9(4)
R_{mag} (%)	10.4	11.7	13.0	12.6	12.5	13.9	13.1

[a] Below 100 K, the preferred magnetic moment orientation is *b* (longest axis), while above 225 K, it is *a* (shortest axis). Due to the availability of high quality data with two wavelengths (1.331 Å and 2.373 Å) at 3.8 K and 300 K, the atomic positions used to refine the 50 K and 100 K moments were taken from the 3.8 K data refinement and the atomic positions used to refine the 225 K, 250 K, and 275 K moments were taken from 300 K data refinement.

Refinements using the data taken above 300 K at HFIR led to moment values which were extremely sensitive to the choice of atomic positions and which did not correspond to the values obtained from the refinement of the C2 low temperature data. For example refinement of the atomic positions and moments at 311 K gave values for the Fe moments on both the O_h and T_d sites which were more than one Bohr magneton smaller and for the Co moments more than one Bohr magneton greater than those found for the C2 data at 300 K. Upon substituting the atomic positions for 300 K (which are not significantly different in terms of the statistical uncertainty), the moment values were reversed between the Fe and Co sites! This problem is likely due to the more restricted Q-range and the somewhat lower signal-to-noise ratio of the HFIR data which compounds the rather highly underdetermined nature of the problem as discussed previously. Nonetheless, there are clear indications from the high temperature data of Figure 7a that not all four magnetic sites order at the same temperature. The temperature dependence below 200 K of the two strongest magnetic reflections, (022) and (102), is of course dominated by the effects of the spin reorientation. Even above 300 K there are anomalies. Consider the temperature dependence of the (102) reflection which shows order parameter like behavior with an approximate critical temperature of ~450 K followed by a plateau to 529 K. In fact the (102) intensity is not observable at 547 K. A similar but less pronounced effect occurs for the (022) reflection near 450 K which is followed by a plateau between 510 K and 547 K. At the maximum temperature, 565 K, the (022) peak is not distinguishable from background, although the counting statistics are poor. This complex behavior should be investigated in more detail with better counting statistics and a finer temperature grid, but the indication of multiple ordering temperatures seems clear.

The bulk magnetic susceptibility data, Figure 8a,b, reflect the effects seen by neutrons. The susceptibility minimum at 100 K and the maximum at 200 K are consistent with the observed spin reorientation. An additional feature is the ZFC/FC divergence below 200 K and the hysteresis which indicates some degree of spin canting. This is confirmed by isothermal magnetization data, Figure 9, that shows hysteresis at 5 K and 200 K. The remnant magnetization is especially well-defined at 200 K. As well, the high temperature susceptibility data show a minimum near 450 K which corresponds to one of the apparent ordering temperatures from the high temperature neutron data. There is a broad maximum at ~570 K, and a reproducible spike at 585 K, close to the maximum magnetic transition from neutron data.

Summary and Conclusions

The mixed B-site brownmillerite, Ca_2FeCoO_5, was synthesized using standard solid state chemistry methods

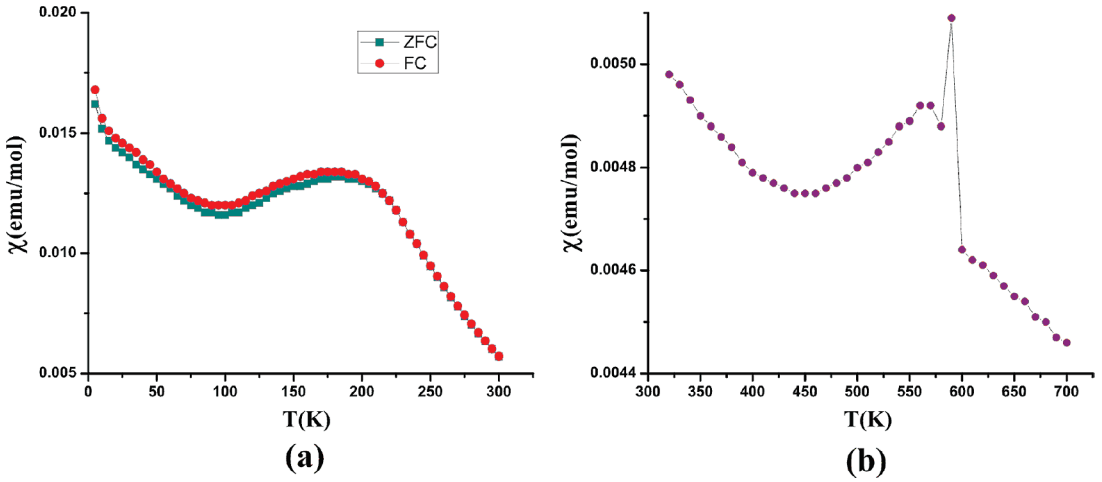

Figure 8. (a) ZFC and FC molar susceptibility data within the temperature range 5−300 K. Note the minimum at ~100 K and the maximum at ~200 K indicative of the spin reorientation found in the neutron data. Also, a ZFC/FC divergence sets in below 200 K, indicating spin canting. (b) Magnetic susceptibility data upon heating the sample from 300 K−700 K. The unusual spike above ~580 K is reproducible. Note the minimum at ~450 K which corresponds to the lower ordering temperature from the neutron study and the broad maximum at ~570 K, close to the maximum ordering temperature from the neutron data.

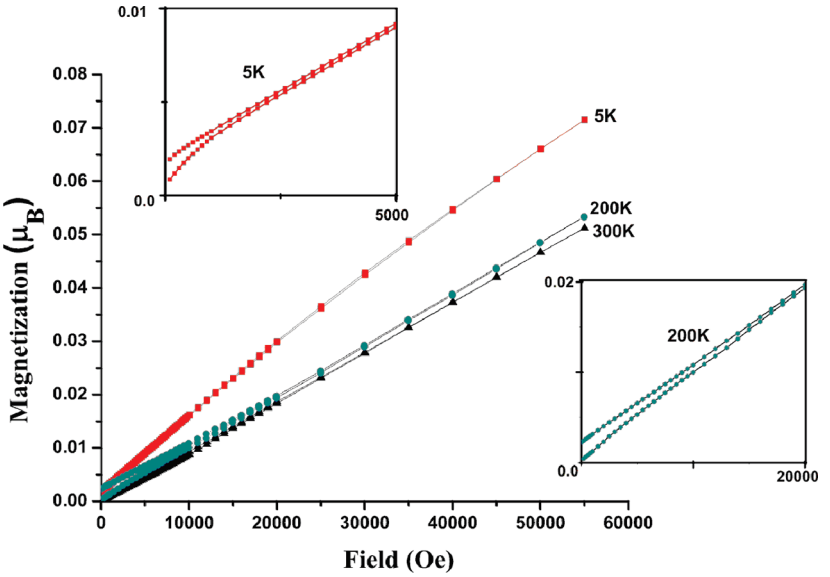

Figure 9. Isothermal magnetization versus applied field for Ca_2FeCoO_5 at various temperatures. Hystereses are observed at 5 K and 200 K, magnified in the insets. The remnant magnetization is especially well pronounced at 200 K.

from which single crystals could be recovered. A number of new phenomena, not seen previously in brownmillerite oxide materials, were observed. It is one of the rare brownmillerite oxides to crystallize in *Pbcm* (*Pcmb*) requiring a supercell with doubling of one of the short axes and with an unique intra- and interlayer ordering of the tetrahedral chains. As well, there are two sets of octahedral and tetrahedral sites. Aided by the strong scattering contrast between Co and Fe for neutrons, an unprecedented intralayer Co/Fe site ordering was seen on the tetrahedral sites. A lesser but still pronounced level of site ordering occurs in the octahedral layers as well leading to an overall NaCl type Fe/Co ordering.

The magnetic structure of this compound was determined to be G-type antiferromagnetic, with both intra- and interlayer antiparallel alignment of spins. A reorientation of magnetic moments, unique to this material, from along the longest axis below 100 K to along the shortest axis above 200 K was observed. The ordered moments for Fe^{3+} and Co^{3+} are significantly smaller than expected for the high spin ions but are similar to those observed in Sr_2FeCoO_5. The high temperature neutron data indicate at least two distinct critical temperatures for long-range magnetic order at ~450 K and ~555 K, suggesting that pairs of the four magnetic sites behave differently. The current data are not sufficiently accurate to assign specific sites to the apparent critical temperatures. Bulk magnetic properties largely reflect the observations from neutron diffraction in terms of the spin reorientation and two ordering temperatures but also indicate spin canting below 200 K.

Acknowledgment. J.E.G. acknowledges the support of the Natural Sciences and Engineering Research Council (NSERC) of Canada through a Discovery Grant. The Canadian Neutron Beam Centre is also supported by NSERC by a Major Facilities Access grant.

The work at the High Flux Isotope Reactor, Oak Ridge National Laboratory (ORNL), was sponsored by the Scientific User Facilities Division, Office of Basic Energy Sciences, U.S. Department of Energy (U.S. DOE). ORNL is operated by UT Battelle, LLC for the U.S. DOE under Contract No. DEAC05-00OR22725.

Supporting Information Available: A CIF file containing the details of X-ray single crystal experiment. This material is available free of charge via the Internet at http://pubs.acs.org.